Appendix D
Example Problems

The examples provided in this appendix clearly demonstrate the procedure for applying the multiple-wedge and single-wedge equations to the stability analysis of wedge systems, stability benefits from uplift reduction, stability benefits of tensioned structural anchors, obtaining shear strength parameters for use in sliding-stability analysis, uplift pressures and differential heads on stilling-basin slabs, and calculating critical wedge-slip angles for selected conditions. The variations of uplift pressure, orientation of failure planes, etc., used in the examples were only selected to simplify the calculations and are not intended to represent the only conditions to be considered during design or investigation of the stability of a hydraulic structure. Dimensions, weights, volumes, densities, forces, and pressures are presented in SI units, with corresponding American units given inside brackets.

D-1. Example D1, Gravity-Dam Sliding Analysis, Single-Wedge System

Determine the factor of safety against sliding for the structure shown in Figure D-1, using the single-wedge sliding analysis method as discussed in Chapter 5 of this EM. As a point of interest, the multiple-wedge analysis would produce the same results for this problem.

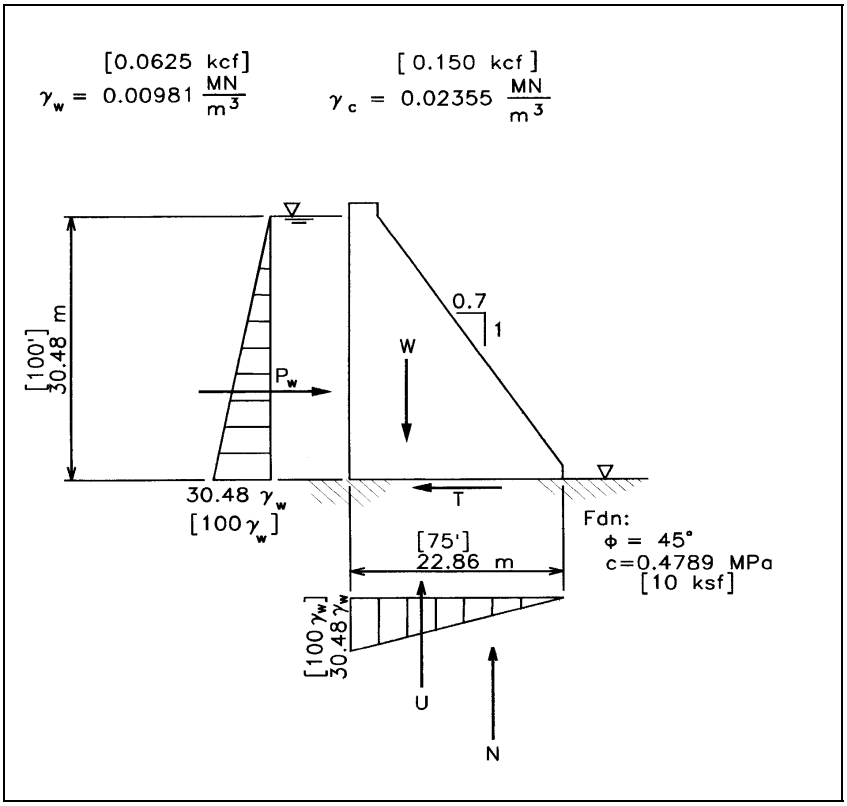

Figure D-1

$$W = 8.812 MN/m [603.8 k/ft]$$

$$T = P_w = \frac{1}{2}\gamma_w h^2 = \frac{1}{2}(0.00981)(30.48)^2 = 4.557 \frac{MN}{m}, [312.5 \text{ k}]$$

$$U = \frac{1}{2}\gamma_w hb = \frac{1}{2}(0.00981)(30.48)(22.86) = 3.418\,\frac{MN}{m}\ [234.38\ \text{k/ft}]$$

$$N = W - U = 8.812 - 3.418 = 5.394\,\frac{MN}{m}\ [369.42\ \text{k/ft}]$$

$$FS = \frac{N \tan\phi + c\,L}{T} = \frac{5.394\ x\ 1 + 0.4789\ x\ 22.86}{4.557} = 3.59$$

D-2. Example D2,Gravity-Dam Sliding Analysis, Multiple-Wedge System

Determine the factor of safety against sliding for the gravity dam shown in Figure D-2. Use the multiple-wedge-sliding analysis as discussed in Chapter 2. The purpose of this example is to illustrate the calculations required for a multiple-wedge sliding analysis using the iterative method.

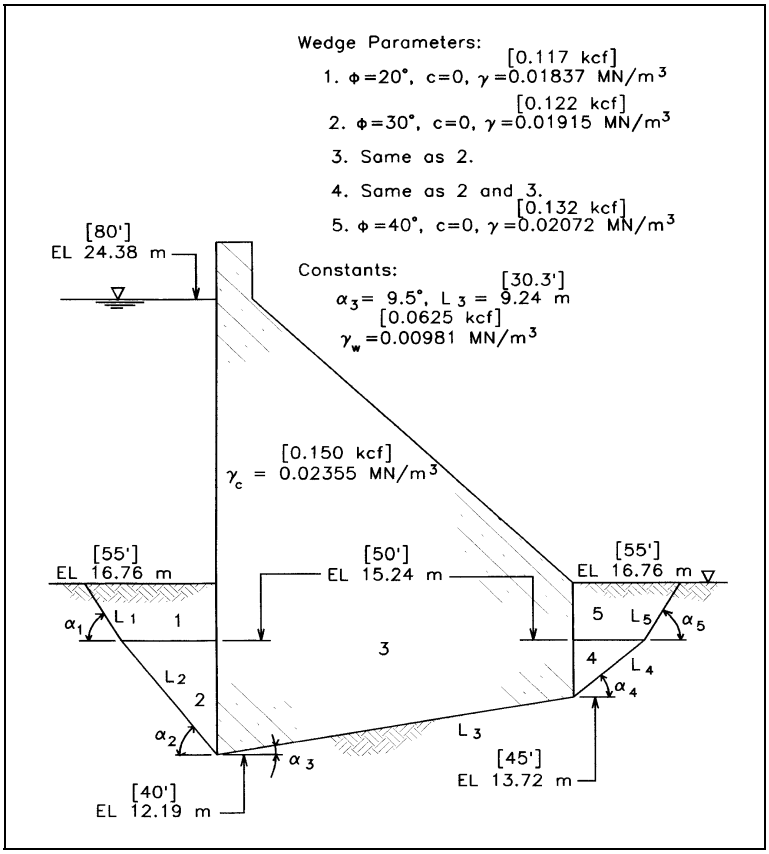

Figure D-2

For an usual load condition, a critical structure, and ordinary site information the minimum-required factor of safety is 2.0. (See Chapter 3).

$$P_{i-1} - P_i = \frac{\left[(W_i + V_i)\cos\alpha_i - U_i + (H_{Li} - H_{Ri})\sin\alpha_i\right]\frac{\tan\phi_i}{FS_i} - (H_{Li} - H_{Ri})\cos\alpha_i + (W_i + V_i)\sin\alpha_i + \frac{c_i}{FS_i}L_i}{\cos\alpha_i - \frac{\tan\phi_i \sin\alpha_i}{FS_i}}$$

Wedge forces for trial safety factor of 1.5

$\underline{i = 1}\ H_{Li} = H_{Ri} = 0, \quad V_1 = 0$

$$\tan\phi_d = \frac{\tan\phi_1}{FS_1} = \frac{\tan 20}{1.5} \qquad \phi_d = \tan^{-1}(0.243) = 13.64°, \quad c_d = 0$$

$$\alpha_1 = -(45° + \frac{\phi_d}{2}) = -51.82°$$

(This orientation is only true if the stratification and surface are horizontal.)

$\sin(-51.82) = -0.786, \quad \cos(-51.82) = 0.618$

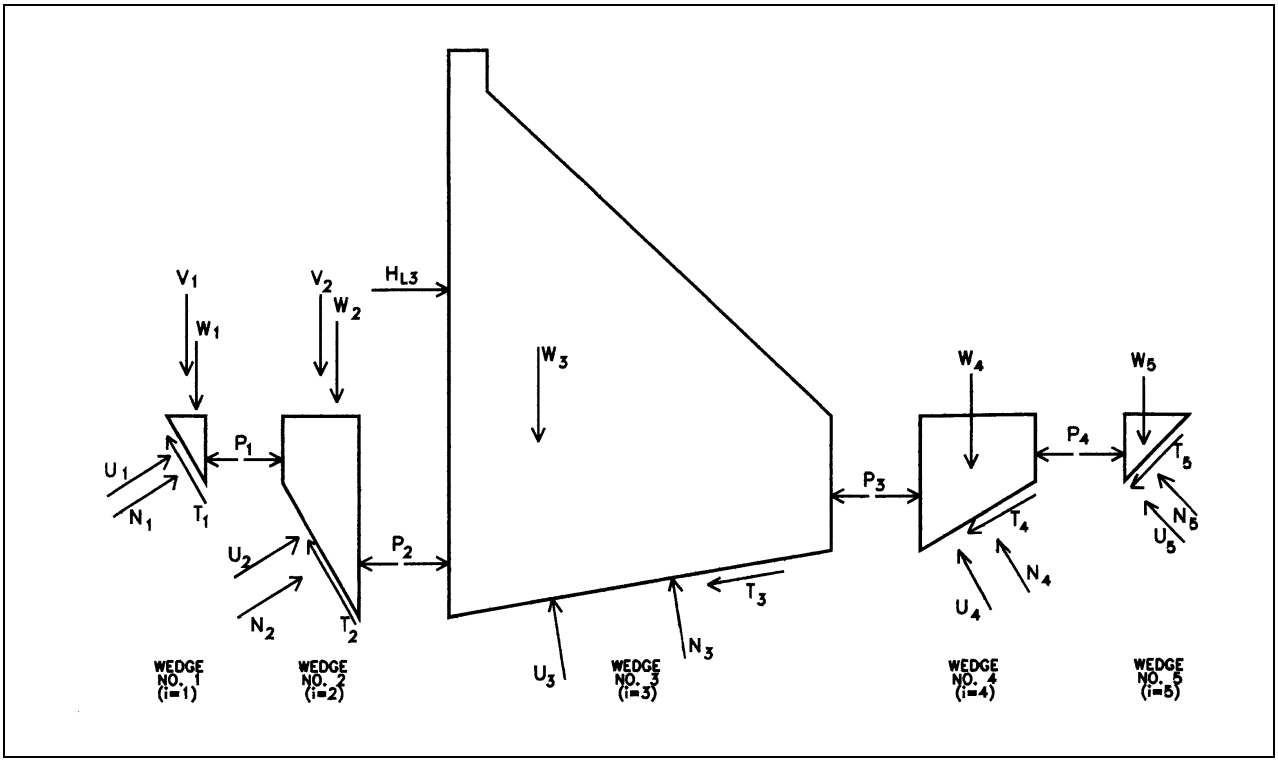

Figure D-3

$L_1 = 1.52 / [\sin(-51.82)] = 1.52 / 0.786 = 1.934\ m\ [6.3'6\ ]$

$$W_1 = \frac{1}{2}(0.00856\ )(1.52\ )(1.934\ )\cos(\ -51.82\ ) = 0.0078\ MN/m\ [0.54\ \text{k/ft}\ ]$$

$$(P_0 - P_1) = \frac{[(0.0078+0)(0.618)-(0-0)(-0.786)]\frac{\tan 20}{1.5} - (0-0)(0.618)+(0.0078+0)(-0.786)+\frac{0(1.934)}{1.5}}{0.618-(\ -0.786\ )\frac{\tan 20}{1.5}} = -0.006\ MN/m\ [-0.42\text{k/ft}]$$

$\underline{i=2}\ H_{L2} = H_{R2} = 0$

$$\tan\ \phi_d = \frac{\tan\ \phi_2}{1.5} = \frac{\tan\ 30}{1.5} \qquad \phi_d = \tan^{-1}(0.385\ ) = 21.05\ °$$

$$\alpha_2 = -(45 + \frac{\phi_d}{2}) = -55.53°$$

$$L_2 = \frac{3.05}{0.8244} = 3.70\ m\ [12.13\ \text{ft}]$$

$$W_2 = 0.00856(1.52)(3.70x0.566) + \frac{1}{2}(0.00934)(3.05)(3.70x0.566) = 0.0571\,MN/m\ [3.91\,\text{k/ft}],\ V_2 = 0,\ c_2 = 0$$

$$\sin(-55.53) = -0.8244 \quad \cos(-55.53) = 0.566$$

$$(P_1 - P_2) = \frac{[(0.0571+0)(0.566)-0+0(-0.8244)]\frac{\tan 30}{1.5} - 0(0.566)+(0.0571+0)(-0.8244)+\frac{0(3.70)}{1.5}}{0.566-(-0.8244\ )\frac{\tan 30}{1.5}}$$

$$(P_1 - P_2) = -0.040\ MN/m\ [-2.69\ \text{k/ft}]$$

$\underline{I=3}\ \alpha_3 = 9.5°\ \ L_3 = 9.270\ m\ [30.3\ \text{ft}],\ c_3 = 0,\ V_3 = 0,\ U_3 = 0.6925\ \text{MN/m}\ [47.34\ \text{k/ft}]$

$$H_{L3} = \frac{1}{2}(0.00981\ )(12.19\ )^2 = 0.7289\ MN/m\ [49.95\ \text{k/ft}\ ]$$

$$H_{R3} = \frac{1}{2}(0.00981)(3.04\ )^2 = 0.0453MN/m\ \ [3.11\ \text{k/ft}]$$

$$H_{L3} - H_{R3} = 0.6836\quad M\quad N\quad /m\quad [46.85\quad \text{k/ft}\ ]$$

$$W_3 = 1.7864\ MN/m\ [122.4\ \text{k/ft}],\ \ \sin 9.5° = 0.165,\ \ \cos 9.5° = 0.986$$

$$(P_2 - P_3) = \frac{[(1.7864 + 0)(0.986) + 0.6836\ (0.165) - 0.6925]\ \frac{\tan 30}{1.5}}{0.986 - 0.165\ x\ \frac{\tan 30}{1.5}}$$

$$\frac{-0.6836\,(0.986) + (1.7864 + 0)(0.165) + \frac{0(9.27)}{1.5}}{0.986 - 0.165\ x\ \frac{\tan 30}{1.5}} \quad = 0.082\ M\ N\ /m\ [5.61\ \text{k/ft}\ ]$$

$\underline{i = 4}\ H_{L4} = H_{R4} = V_4 = 0, \quad c_4 = 0$

$$\tan \phi_d = \frac{\tan \phi_4}{FS_4} = \frac{\tan 30°}{1.5} \qquad \phi_d = \tan^{-1}(0.385\ ) = 21.05°$$

$$\alpha_4 = 45 - \frac{\phi_d}{2} = 34.475° \quad \sin(34.475) = 0.566 \quad \cos(34.475) = 0.824$$

$$L_4 = \frac{1.52}{\sin 34.475} = 2.685\ m\ [8.8'3]$$

$$W_4 = (0.01091)(1.52)(2.685\ x\ 0.824) + \frac{1}{2}(0.00934\ )(1.52)(2.685\ x\ 0.824) = 0.0524\ M\ N\ /m\ [3.59\ \text{k/ft}]$$

$$(P_3 - P_4) = \frac{[(0.0524 - 0)(0.824) - 0 + 0(0.566)]\ \frac{\tan 30}{1.5} - 0(0.824) + (0.0524 + 0)(0.566\ ) + \frac{0(2.865)}{1.5}}{0.824 - 0.566\left(\frac{\tan 30}{1.5}\right)}$$

$(P_3 - P_4) = 0.076\ MN/m\ [5.23\ \text{k/ft}\ ]$

$\underline{i = 5}\ H_L 5 = H_{R5} = V_5 = 0, \quad c_5 = 0$

$$\tan \phi_d = \frac{\tan \phi_5}{FS_5} = \frac{\tan 40}{1.5} \qquad \phi_d = \tan^{-1}(0.559\ ) = 29.22°$$

$$\alpha_5 = 45 - \frac{\phi_d}{2} = 30.38° \quad \sin 30.38 = 0.5058 \quad \cos 30.38 = 0.8626$$

$$L_5 = \frac{1.52}{\sin 30.38} = 3.01\ m\ [9.89\ \text{ft}\ ]$$

$$W_5 = \frac{1}{2}(0.01091) \quad (1.52) \quad (3.01 \quad \_ \quad 0.8626) \quad = 0.0215 \quad M \quad N \quad /m \quad [1.48 \quad \text{k/ft} \quad]$$

$$(P_4 - P_5) = \frac{[(0.0215+0)0.862\ ) - 0 + 0(0.506)]\frac{\tan 40}{1.5} - 0(0.863) + (0.0215+0)(0.506) + \frac{0(3.01)}{1.5}}{0.863 - 0.506\left(\frac{\tan 40}{1.5}\right)}$$

$$(P_4 - P_5) = 0.036 \quad MN/m \quad [2.51 \quad \text{k/ft} \quad]$$

Summing the resultant horizontal forces for all wedges:

$$(P_0 - P_1) + (P_1 - P_2) + (P_2 - P_3) + (P_3 - P_4) + (P_4 - P_5) = -0.006 - 0.040 + 0.082 + 0.076 + 0.036 = 0.148 > 0$$

Since this summation is greater than zero, the safety factor (FS) must be greater than 1.5. Calculations have been made for trial safety factors of 2.5 and 2.0 in a similar manner, and the results are presented in Tables D-2 through D-4 and on a graph.

Table D-2 FS = 1.5

i	α	L	H_L	H_R	V	W	U	$P_{I-1} - P_i$
1	-51.82	1.934	0	0	0	0.0078	0	-0.006
2	-55.53	3.700	0	0	0	0.0571	0	-0.040
3	9.5	9.270	0.7289	0.0453	0	1.7864	0.6925	0.082
4	34.47	2.685	0	0	0	0.0524	0	0.076
5	30.38	3.010	0	0	0	0.0215	0	0.036

$\sum \Delta P = 0.148$

Table D-3 FS = 2.5

I	α	L	H_L	H_R	V	W	U	$P_{i-1} - P_i$
1	-49.14	2.015	0	0	0	0.0086	0	-0.007
2	-51.50	3.895	0	0	0	0.0661	0	-0.053
3	9.5	9.270	0.7289	0.0453	0	1.7864	0.6925	-0.112
4	38.50	2.438	0	0	0	0.0452	0	0.057
5	36.72	2.609	0	0	0	0.0169	0	0.024

$\sum \Delta P = -0.091$

Table D-4 FS = 2.0

I	α	L	H_L	H_R	V	W	U	$P_{i-1} - P_i$
1	-50.16	1.984	0	0	0	0.0083	0	-0.007
2	-53.05	3.813	0	0	0	0.0625	0	-0.047
3	9.50	9.270	0.7289	0.0453	0	1.7864	0.6925	-0.041
4	36.95	2.538	0	0	0	0.0479	0	0.064
5	33.62	2.752	0	0	0	0.0189	0	0.028

$\sum \Delta P = -0.003$

The safety factor for sliding equilibrium of the five-wedge system is determined from:

$\sum_{i=1}^{5} (P_{i-1} - P_i) = \Delta P_R \quad \Delta P_R = 0$ which gives the safety factor for equilibrium.

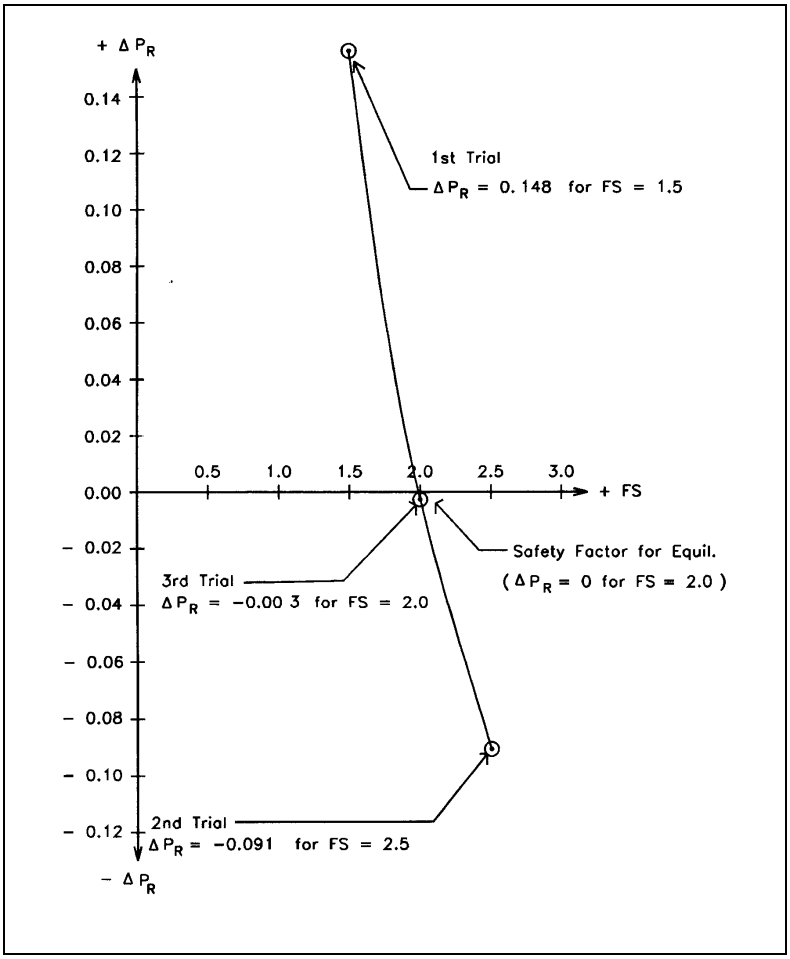

Figure D-4 Graphical solution for safety factor

D-3. Example D3, Lock Monolith on Rock.

Perform a complete stability analysis for the lock chamber wall monolith shown in Figure D-5. The structure classification is *normal*, the loading is a *usual* condition, and site information is *ordinary.* Assume that a vertical crack exists from the top of the rock to the base of the wall on the driving side. It is also assumed that movement of the wall will not be sufficient for any significant rock force to develop on the resisting side. From Chapter 3, the minimum factor of safety against sliding for a *usual* load condition, a normal structure classification, and *ordinary* site information is 1.50.

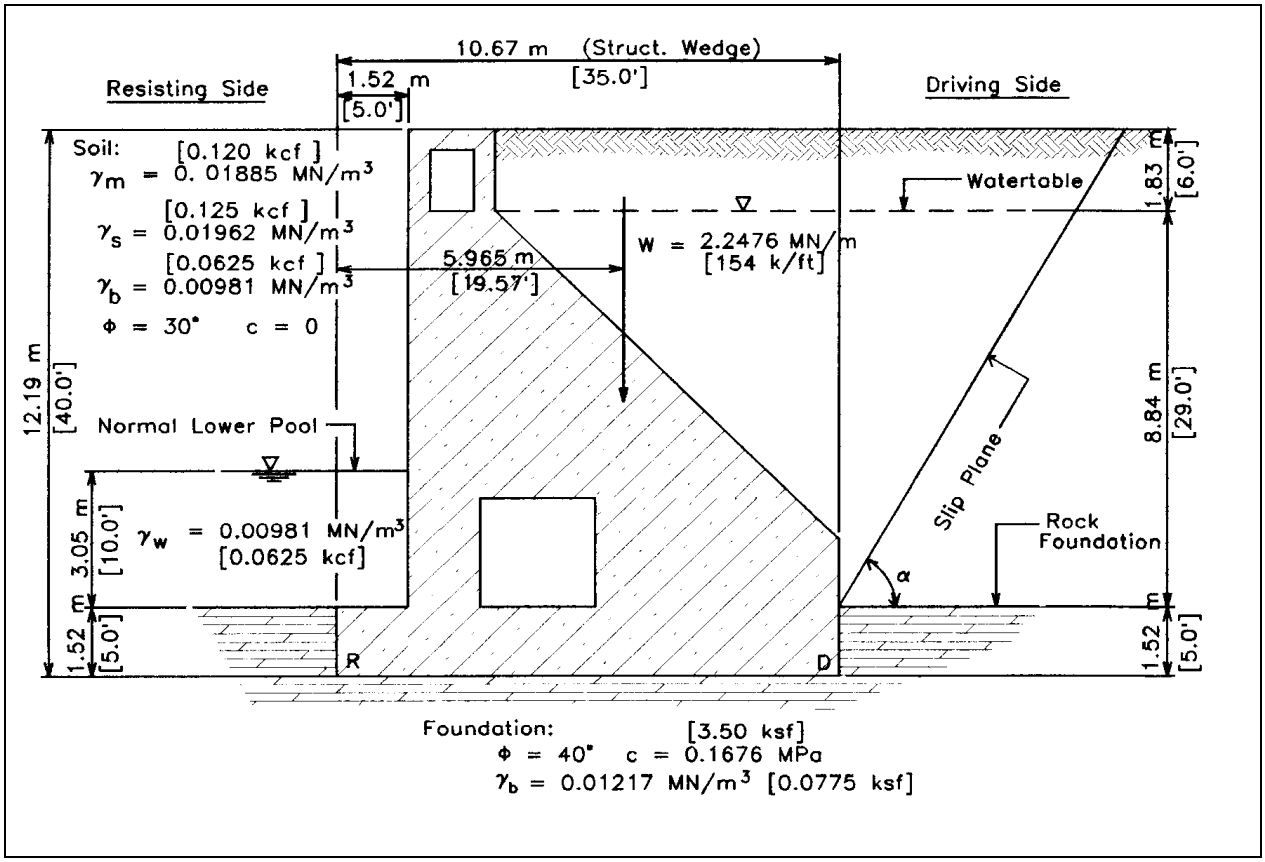

Figure D-3

a. *Driving Side, Lateral Water Force*

$$p_s = K\,\gamma_m(\,h - h_s\,) \quad p_s = 0.4714 \times 0.01885 \times 1.83 = 0.01626\ M\ N\ /m\,(0.3395\ \text{ksf})$$

$$P_w = \frac{1}{2}\gamma_w h_s^2 = \frac{1}{2}(0.00981)(\ 10.36\ )^2 = 0.5265\ M\ N\ /m\ [36.13\ \text{k/ft}\,]$$

b. Driving Side, Soil

$$\phi_d = \tan^{-1}\left(\frac{\tan 30^\circ}{1{,}50}\right) = 21.05^0, \quad K = \tan^2\left(45^\circ - \frac{\phi_d}{2}\right) = 0.4715$$

$$p = K[\gamma_m h - (\gamma_m - \gamma_b)h_s] \quad p = 0.4715[0.01885 \times 10.67 - (0.01885 - 0.00981)884$$

$$p = 0.05715 MPa (1.1933 ksf)$$

$$P = \frac{1}{2}(0.01626)(1.83) + \frac{1}{2}(0.01626 + 0.05715)8.84 = 0.3394\ M\ N\ /m\ [23.26\ \text{k/ft}]$$

c. *Resisting Side Lateral Water Force*

$$P_w = \frac{1}{2}\, x\, 0.0448\, x\, 4.57 = 0.1024\ MN/m\ (7.03\ k/ft)$$

d. Uplift

$$u_R = \gamma_w h_s = 0.00981\ x\ 4.57 = 0.0448, \quad u_D = 0.00981\ x\ 10.36 = 0.1016$$

$$U = 1/2\ (0.0448 + 0.1016)(10.67) = 0.7810\ MN/m\ (53.53\ k/ft)$$

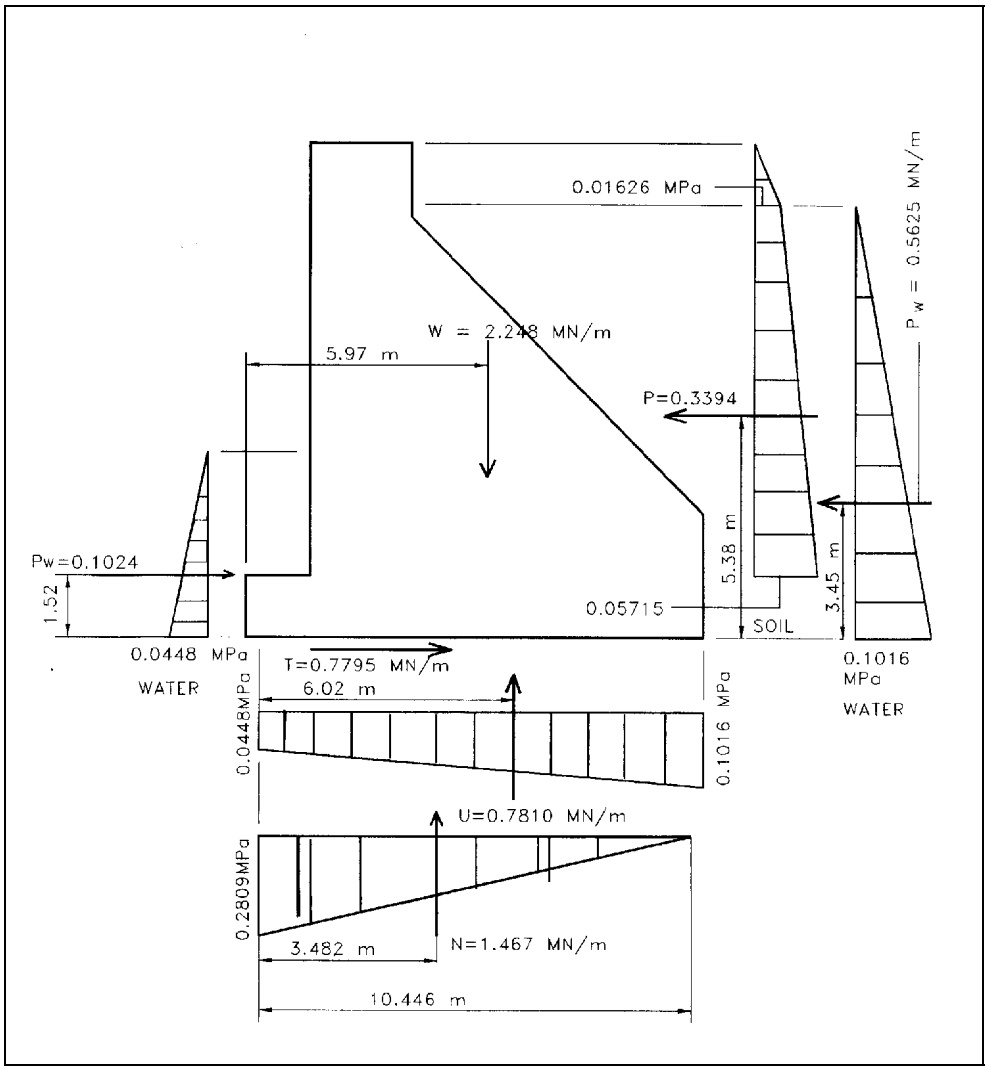

Figure D-6 Forces and pressures from single wedge analysis

e. Resultant Location for Single Wedge Sliding Analysis (see Figure D-6)

$$\Sigma M_R = 2.248x5.97 + 0.1024x1.52 - 0.3394x5.38 - 0.5265x3.45 - 0.7810x6.02 = 5.108$$

$$N = 2.248 - 0.781 = 1.467\ MN/m, \quad X_R = \frac{\Sigma M_R}{N} = 3.482\ m, \quad L = 3\,X_R = 10.446\ m < 10.67\ m$$

$$FS = \frac{N \tan\phi + cL}{T} = \frac{1.467x0.8391 + 0.1676x10.67}{0.4483} = 6.63 > FS_{sliding} = 1.50$$

f. *Results.* Factor of Safety Against Sliding Exceeds the Minimum Requirement. 97.9 % of base is in compression, but Resultant Location Criteria is assumed to be satisfied since any rock resistance has been neglected. Uplift will not be re-calculated

D-4. Example D4, Stability Benefits from Uplift Reduction

This example problem represents a non-overflow section (gravity dam), which is part of a hydroelectric power generating project. The non-overflow section was designed in the early 1900s under the assumption of full uplift acting over 50 percent of the base. Stability analyses performed under current stability criteria indicates the structure does not meet resultant location, and sliding factor of safety requirements. The dam section has a grouting and drainage system, and piezometer readings indicate uplift downstream of the drains is at or near tailwater. Maximum drain efficiency allowed for the design of new dams is 50 percent according to information provided in Appendix C. The stability will be evaluated using 50-percent drain efficiency. It will also be evaluated assuming 90-percent drain efficiency, which conservatively represents the degree of drain efficiency indicated by piezometer readings taken over the past 40 years.

a. Dam Configuration. A cross section through the highest section of the dam is shown in Figure D7. The pool conditions are indicated for the normal operating condition. A *usual* loading condition is used in establishing the required factors of safety for sliding and resultant location.

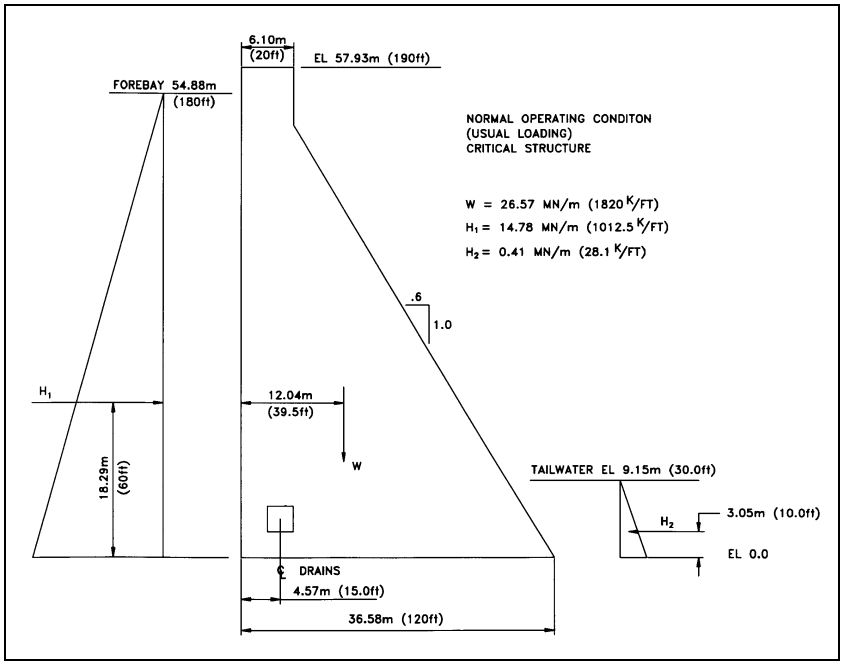

Figure D-7

b. Foundation strength parameters. Through explorations and testing it has been determined that the angle of internal friction for the foundation (ϕ) is 55-deg, and because the foundation rock is highly jointed and fractured, the cohesive strength (c) is assumed to be zero.

c. Loads. The forebay and tailrace pool elevations representing the usual loading condition are shown in Figure D-7. Table D-5 provides a summary of the loads and a summary of the moments of the loads about the heel of the dam.

d. Uplift. The uplift pressures and resultant locations for the 50-percent drain efficiency condition are shown in Figure D-8, and for the 90-percent drain efficiency in Figure D-9. The forebay pool, since this is a hydroelectric power generating facility, is usually kept at elevation 54.88 m (180 ft) to maximize power benefits. Piezometer measurements and records have been kept over the last 40 years. Many records are available for the forebay pool at elevation 54.88 m (180 ft) and with tailwater at a maximum elevation of 9.15 m (30.0 ft). The records indicate the uplift downstream of the drains remains at or near tailwater. The records also indicate that uplift pressures are not increasing with time. A comparison of the 90-percent drain efficiency condition with the actual measured uplift pressure condition for the normal operating forebay pool / maximum tailwater condition is shown in Figure D-10. It is apparent that the 90-percent drain efficiency condition conservatively represents the actual foundation uplift pressures.

Table D-5 Loads and Moments (without uplift)

Load Designation	Horizontal Load (MN)	Vertical Load (MN)	Moment Arm (meters)	Moment @ A (MN-meters)
H_1	14.78		18.29	270.33
H_2	-0.41		3.05	-1.25
W		26.57	12.04	319.90
SUM	14.37	26.57		588.98

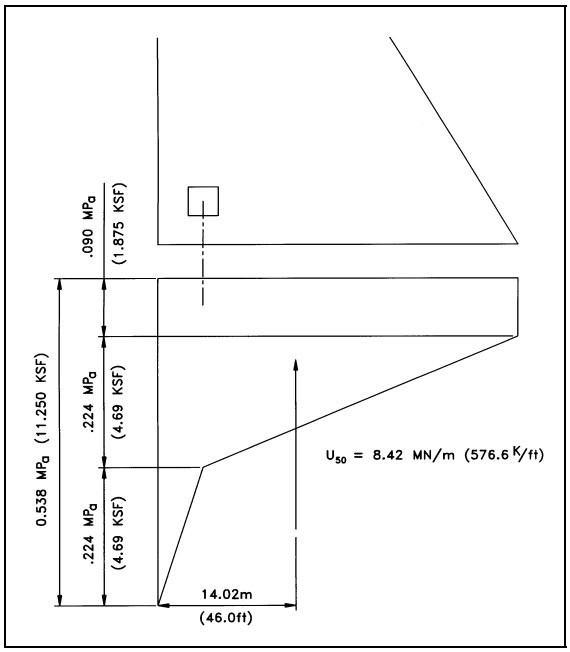

Figure D-8 Uplift with 50 percent drain efficiency (Resultant in middle 1/3 of base)

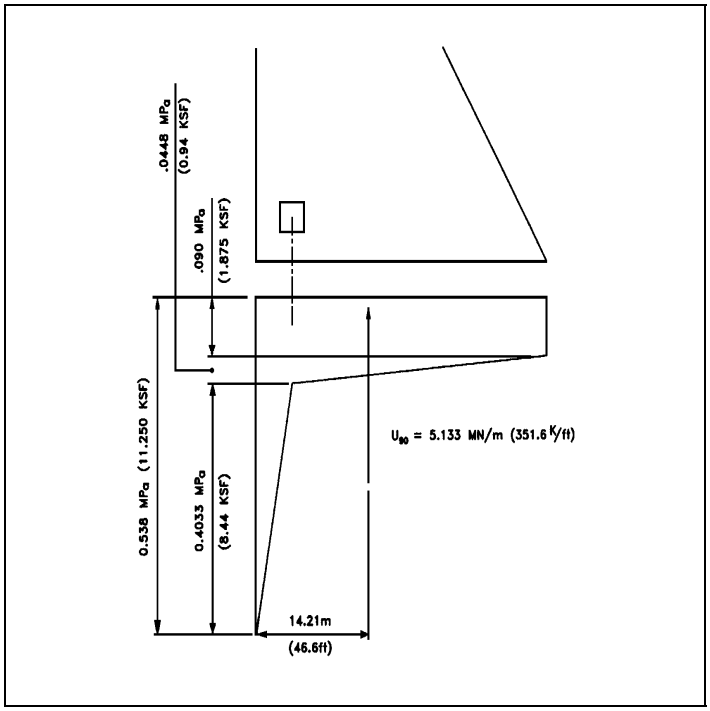

Figure D-9 Uplift with 90 percent drain efficiency

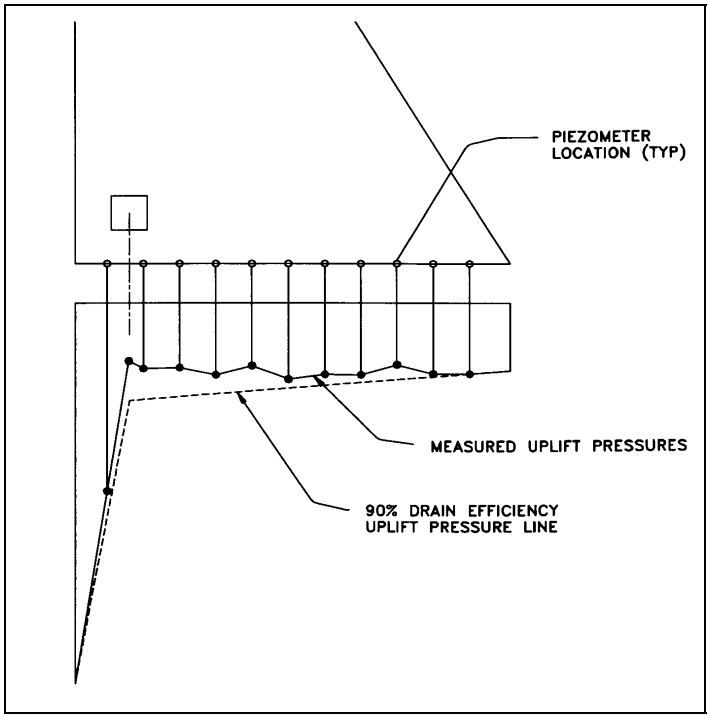

Figure D-10 Measured uplift versus 90% drain efficiency

e. Sliding Factors of Safety. The sliding factors of safety are calculated using the limit equilibrium method. For the single-plane failure surface condition with a horizontal failure plane, the factor of safety equation becomes:

$$FS = \frac{cA + (V\ U)\tan\phi}{H}\ \text{, and}$$

For the 50-percent drain efficiency condition:

$$FS = \frac{18.15\tan 55}{14.37} = 1.80 < 2.00 \quad \text{N.G.}$$

For the 90-percent drain efficiency condition:

$$FS = \frac{21.44\tan 55}{14.37} = 2.13 > 2.00 \quad \text{O.K.}$$

f. Conclusions. The use of a drainage efficiency of 90-percent provides the required factor of safety for sliding, whereas for the 50-percent drainage efficiency condition the structure fails to meet sliding requirements. This particular example problem illustrates the case where the use of existing uplift conditions can eliminate the need for a costly stability retrofit. A prudent designer, however, would make sure that the drains were inspected and cleaned on a regular basis, that there were sufficient piezometers throughout the base of the structure, and that these piezometers were read on a regular basis to remove all concerns over high uplift pressure leading to stability problems. There are many cases where drainage systems for dams have reduced uplift pressures to tailwater levels.

D-5. Example D5, Sliding of Gravity Dam With and Without Tensioned Structural Anchors

This example illustrates how sliding stability is enhanced by the use of tensioned structural anchors. The anchors accomplish stability by decreasing the component of the resultant force that acts parallel to the sliding plane and by increasing the component of the resultant force that acts normal to the sliding plane. Foundation strength parameters used in this example are $\phi = 40^{o}$ and c=0. Force diagrams are shown in Figures D-11 and D-12.

Without Anchors.

N = W - U = 5.04-1.48 = 3.56 MN/m(243.28 k/ft); T = ΣH = 2.23 MN/m(153.1 k/ft)

$$F\ S = \frac{N\ \tan\ \Phi}{T} = \frac{(3.56)(0.8391)}{2.23} = 1.34\ < 2.0\ \text{N .G .}$$

With Anchors.

$$N = W + F\sin 45° - U = 5.04 + (1.21)(0.707) - 1.28 = 4.61\ M\ \ N/m\ (315.9\ \text{k/ft})$$

$$T = 2.23 - F\cos 45° = 2.23 + (1.21)(0.707) = 1.38\ M\ \ N/m\ (94.6\ \text{k/ft})$$

$$FS = \frac{N\tan\phi}{\text{T}} = \frac{4.61\ x\ 0.8391}{1.38} = 2.80 > 2.0\ \text{O.K .}$$

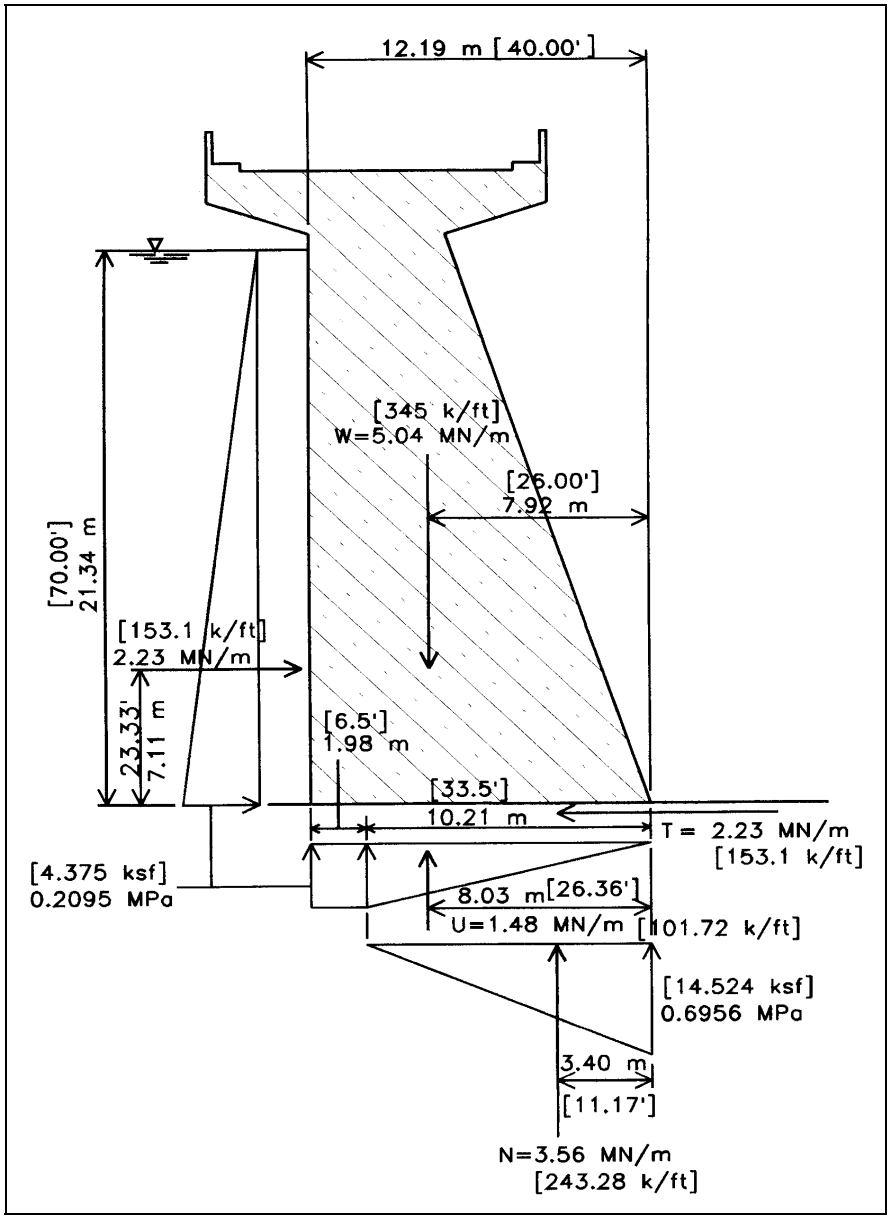

Figure D-11. Stability without tensioned structural anchors

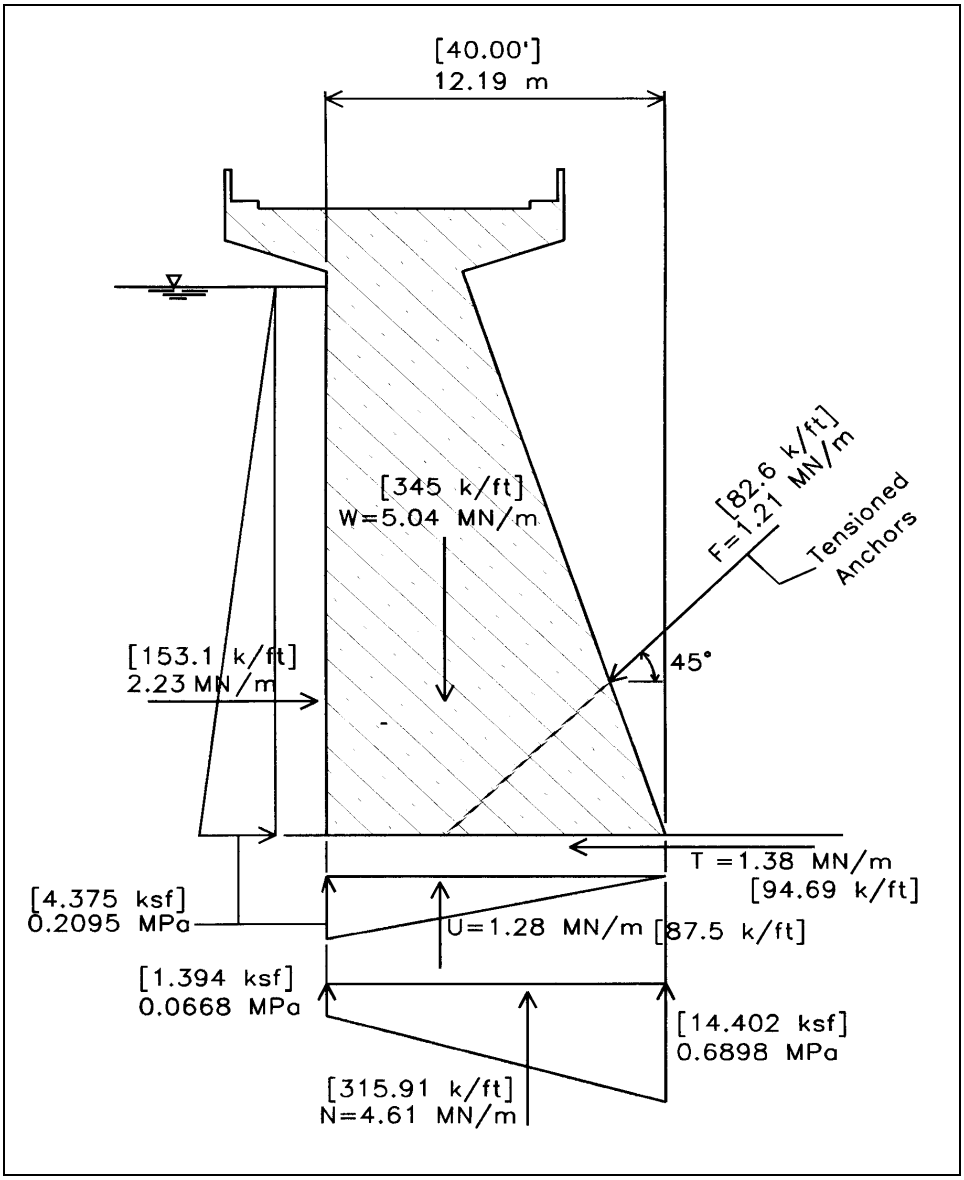

Figure D-12. Stability with tensioned structural anchors

D-6. Example D6, Obtaining Shear Strength Parameters for Use in Sliding-Stability Analyses

The limit equilibrium approach, used for determining a sliding factor of safety, will only provide meaningful results when there is a high degree of confidence that the shear strength parameters used are a conservative representation of actual foundation strengths. The selection of the shear strength parameters involves a great deal of uncertainty. Shear strength parameters can be determined through laboratory and in situ testing, by empirical methods, or by judgment based on a knowledge of rock mechanics and geological conditions. The type of methods and testing used depends on whether the sliding failure plane consists of intact rock, jointed rock, or sheared rock zones containing a weak filler material. Although laboratory testing is the most common way of determining shear strength parameters, the strength of laboratory samples may or may not be indicative of the strength of the prototype. In general, due to size effects, the laboratory samples will provide strengths greater than that of the prototype.

a. Stress / Strain Relationships. There is no consideration of strain in the limit equilibrium method. For foundations that contain more than one material, or are made up of a combination of intact rock and jointed or sheared rock, the limit equilibrium method is only valid when the materials behave in a typical elastic-plastic manner. This means that once the intact rock reaches its peak shear strength, the strains necessary to reach the peak strengths of the jointed and sheared materials can be obtained without a loss of strength through strain softening in the intact rock. For strain softening situations, some judgments must be made with respect to the selection of strength parameters which represent failure strain conditions.

b. Zintel Canyon Project – Foundation Materials. The Foundation and Seepage Analysis Report for the Zintel Canyon Project is used to illustrate the foundation strength determination process for a dam constructed on jointed basalt with various degrees of weathering. The descriptions of the various materials, which make up the foundation, and the laboratory test results, are described below. This information was taken directly from the referenced report.

(1) General. The materials mapped in the foundation of Zintel Canyon Dam consist of a basalt bedrock. The basalt is moderately to intensely weathered and has been subjected to heat alteration and shearing. Shears were mapped in the left abutment, stilling basin, and key trench.

(2) Slightly to moderately weathered basalt. Approximately 20 percent of the total foundation area of Zintel Canyon Dam consists of slightly weathered to moderately weathered basalt. The closely jointed rock resulted in a rough foundation surface with tightly interlocked angular pieces of basalt extending 152.4 mm (6-in.) or more above the lowest portions of the cleaned foundation surface. Drill hole DH-6RD was completed in the slightly to moderately weathered basalt in the right abutment area. Core samples recovered from this hole consisted of closely jointed, hard basalt. The bi-axial shear tests results on the core samples are shown in Figure D-13.

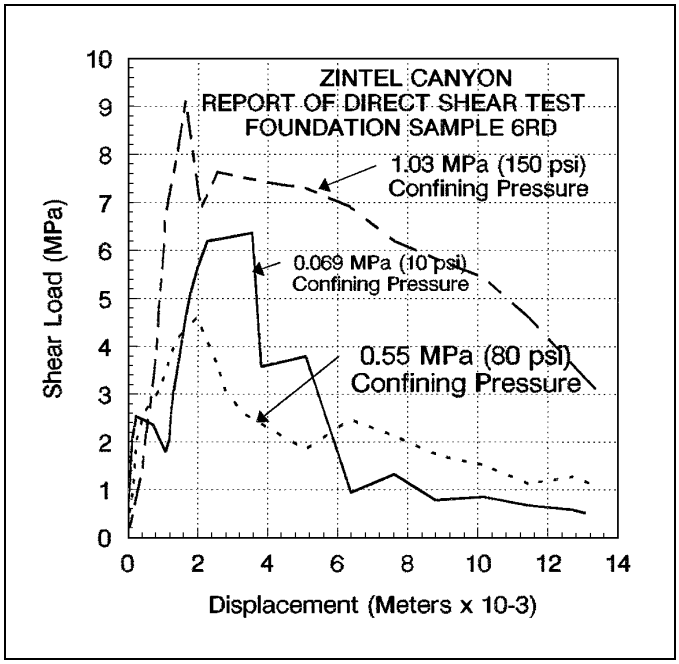

Figure D-13. Direct shear test for slightly to moderately weathered basalt

(3). Moderately to intensely weathered basalt. Approximately 55 percent of the total foundation of Zintel Canyon Dam consists of moderately weathered to intensely weathered basalt. The higher degree of weathering, and very close fracturing in these areas of the foundation, resulted in angular pieces of the basalt being easily loosened and requiring removal during foundation cleaning. The more weathered condition of the basalt resulted in a somewhat more irregular foundation surface than in the slightly to moderately weathered areas. Drill hole DH-1SB was completed in a typical area of the moderately weathered to intensely weathered basalt. Core samples from this hole consisted of very closely fractured and jointed weathered basalt. The bi-axial shear test results on the core samples are shown in Figure D-14.

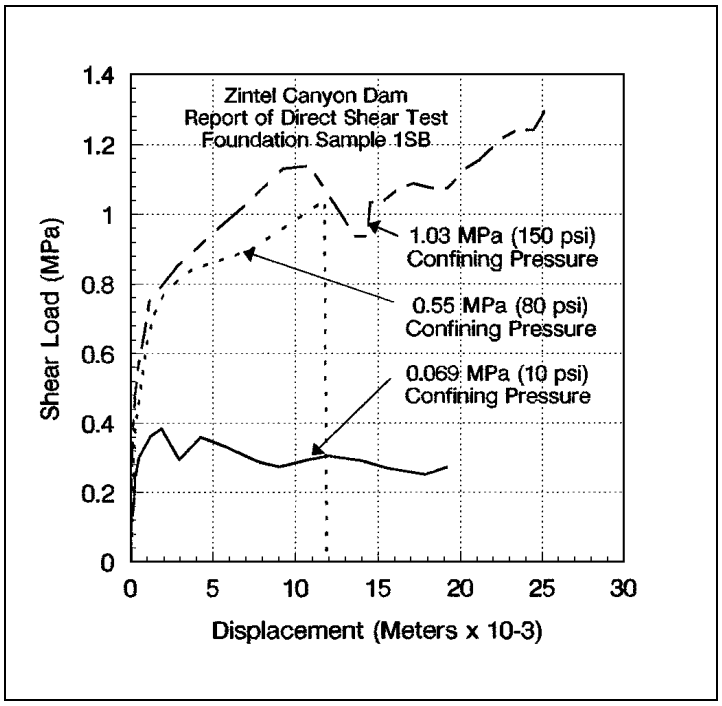

Figure D-14. Direct shear test for moderately to intensely weathered basalt

(4) Intensely weathered / altered basalt. The intensely weathered / altered basalt comprises approximately 20 percent of the total area of the dam foundation. The condition of the rock varies throughout the mapped areas. Commonly, the weathering and alteration resulted in a foundation surface characterized by gravel-sized loosely interlocked angular pieces of basalt extending less than 76.2 mm (3-in.) above the lowest portions of the cleaned foundation. However, some limited areas of the intensely weathered and highly altered basalt are characterized by fragments within a matrix of soil-like highly altered and decomposed basalt. The highly altered areas of the foundation were excavated somewhat deeper than the surrounding areas. However, there was no indication the material was improving with depth, or that by excavating deeper the material would improve. Drill hole DH-1SB, completed in the right side of the stilling basin, encountered the intensely weathered and altered basalt. Core samples from this hole were disturbed during the drilling operation and were primarily recovered as angular basalt fragments. On the basis of the recovered core samples and foundation observations, the intensely weathered and altered areas of the foundation generally consist of a poorer-quality rock than in the moderately to intensely weathered areas, but better-quality rock than in the sheared areas where a large percentage of the cored material was recovered as basalt fragments in a matrix on clay or silt. Therefore, the shear strength of the basalt in the intensely weathered and altered areas of the foundation is considered to be somewhat higher than in the sheared areas.

(5) Shear zones. Shears make up approximately 5 percent of the total foundation of Zintel Canyon Dam. Shears were mapped in the left abutment, stilling basin, and key trench. The shears are predominantly high angle and are mostly orientated from North 5-deg West to North 46-deg East. With this orientation, the shears do not appear to threaten the safety of the structure. There is no indication that the shears would intercept one another at shallow depths, creating the potential for a block failure, or that they form planes of significant weakness in the foundation. Also, due to the infilling of clay and/or silt within the shears, the shear planes are not expected to provide pathways for seepage under the dam. The shears primarily consist of sand - to-gravel-sized fragments of basalt in a matrix of clay or silt. The sheared foundation surface areas are somewhat smoother than other areas of the foundation. Drill hole DH-7LD, located near the base of the left abutment was completed in the area of shear S-9. The core samples from this hole consisted of angular to sub-angular fragments of basalt in a clay matrix. The bi-axial shear test results on the core samples are shown in Figure D-15.

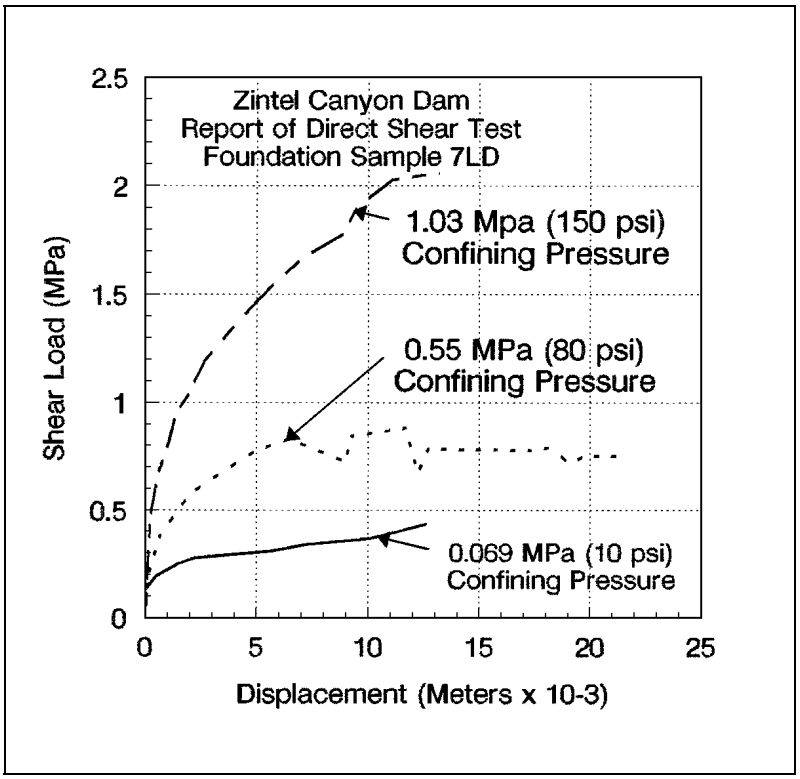

Figure D-15 Direct-shear test for shear zone material

c. Foundation samples and laboratory test results.. Foundation core samples from drill holes, DH-1SB, DH-6RD and DH-7LD were prepared for bi-axial direct-shear strength tests. Sample selections were dependent on core condition (absence of drilling and handling disturbance). In addition, the samples were selected so that the typical best, average, and poorest quality foundation rock encountered would be tested..

(1) Bi-axial shear sample preparation and test procedure. Bi-axial direct-shear strength tests were performed at confining pressures of 1.03, 0.55, and 0.069 MPa (10, 80, and 150 psi.). A test section of 0.762 to 0.915 m (2.5 to 3.0 ft) per hole (two sections in DH-7LD) was selected. In general, each bi-axial shear strength specimen was saw cut to a nominal 0.2033 m (8-in.) length, placed in steel shear blocks, plastered in place and tested. Rock cores from drill holes DH-1SB and DH-7LD could not be handled without breaking apart, so specimens from these holes were prepared by wire-banding the original PVC encasement around the core and saw-cutting through both the PVC and the rock core. Specimens from drill hole DH-1SB required a wax coating in order to keep the samples intact after removal from the PVC encasement prior to placing in the shear blocks. Bi-axial testing was determined to be the most practical method for testing this material. Tri-axial testing was not considered appropriate. The required sample preparation and significant handling requirements made it highly unlikely that an undisturbed rock sample could be situated in the available tri-axial chamber. It is recognized that tri-axial testing of poorer-quality rock would yield improved shear performance, if an undisturbed sample could have been prepared.

(2) Test results. Load-displacement curves from the bi-axial shear tests are shown in Figures D-13 through D-15, and the results in terms of shear strength versus confining pressure are plotted in Figure D-16. The rock samples describes as hard basalt, minor fractures (DH-6RD), representing approximately 20 percent of the foundation rock yielded a cohesive value of 1.6552 MPa (240 psi) and angle of internal friction of 82 deg. The rock samples described as severely fractured, weathered basalt, minor infilling (DH-1SB), representing approximately 55 percent of the foundation rock yielded a cohesion value of 0.414 MPa (60 psi) and an angle of internal friction of 39 deg. The rock samples described as weathered sheared basalt, fully infilled with altered clay / sand (DH-7LD), representing 5 percent of the foundation rock yielded a cohesion value of 0.0897 MPa (13 psi) and an angle of internal friction of 56 deg. The test results from several of the shear tests were not peak values of shear load. They were actually the value of shear when the test was concluded.

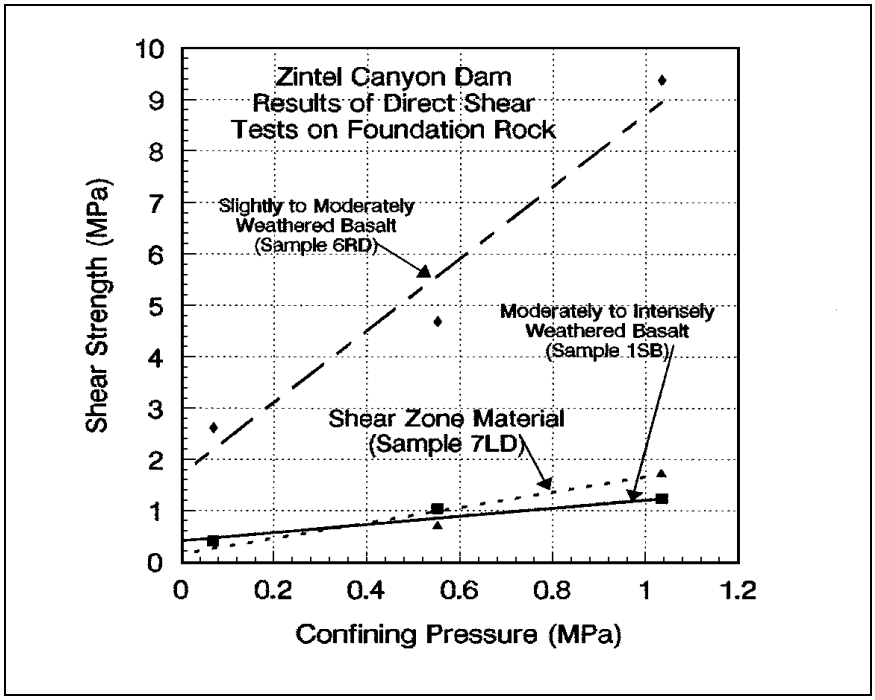

Figure D-16 Shear strength versus confining pressure

d. Observations. The example problem is used to illustrate the difficulties in establishing foundation strength parameters for foundation rock that is jointed and sheared. Intact foundation rock generally poses no problems in the selection of strength parameters, because even with extremely conservative values the foundation has no difficulty in carrying the loads imposed on it by the structure. As it can be seen from the Zintel Canyon Dam direct-shear load / displacement curves, the foundation often exhibits strain-softening characteristics rather than the elastic-plastic characteristics assumed in the limit-equilibrium method. Therefore, the stress/strain relationships of the various foundation materials play an important part in the selection of strength parameters to be used in the sliding stability analysis. This example also demonstrates how erratic the tests results can be and how difficult it can be to establish a single set of strength parameters from the test results. For Zintel Canyon Dam, conservative lower-bound shear-strength values representing the sheared basalt material provided a sliding factor of safety greater than required. Because lower-bound shear-strength parameters were used in the sliding stability analysis, a normal site information factor was selected to establish the required factor of safety.

D-7. Example D7, Spillway Slab With And Without Untensioned Structural Anchors.

This example compares the spillway slab thicknesses required to withstand flotation, with and without the use of untensioned structural anchors. The analysis is for a condition referred to as *rapid drawdown*, which occurs when the spillway gates are closed suddenly. This results in the entrapment of uplift pressure under the slab for a short period of time while the actual water surface is near or at the top surface of the slab. In this example, the entrapped uplift head is assumed to be 3.049m + t ([10 ft + t]). The plan and elevation of the spillway slab panel used in this example are shown in Figure D-17. It is assumed for this example that the return period for the loading condition results in an *unusual* loading condition classification, *normal* importance classification, and *normal* site information.

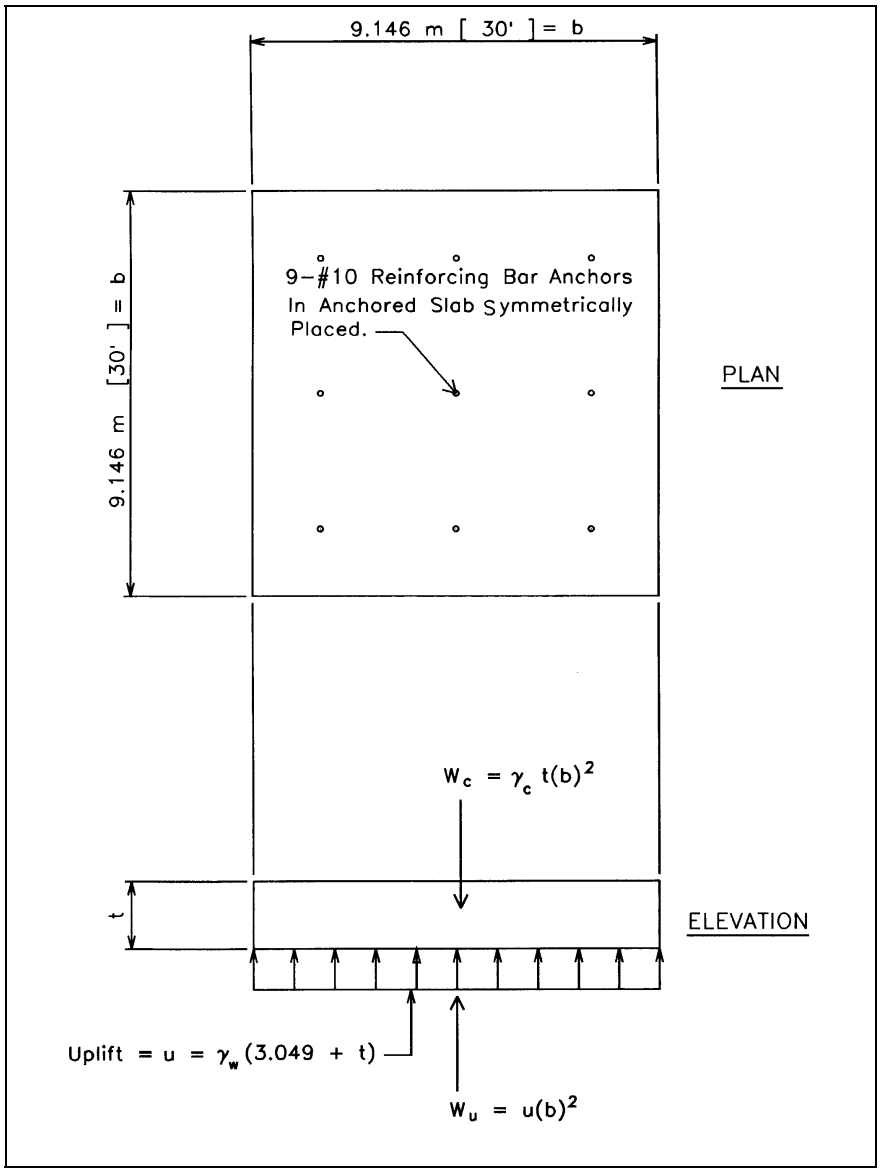

Figure D-17 Anchored spillway slab

a. Thickness with anchors.

$$W_u = \gamma_w (3.049 + t)\, b^2 = 0.00982\,(3.049 + t)(9.146)^2 = 2.50456 + 0.82144\, t$$

$$W_c = \gamma_c\, b^2\, t = 1.97078\, t$$

The requirement of EM 1110-2-2104 for adequacy of reinforcing bar is $\phi R \geq U$ where $\phi = 0.9$ for tension. Thus:

$$U = 0.75[1.3(1.7\, W_u - 1.4\, W_c)], \quad R = N\, A_s\, f_y$$

$$U = 0.75\,(1.3\,[1.7\,(2.50\,4\,5\,6 + 0.82144\,t) - 1.4\,(1.97078\,t)])$$

$$U = 4.15131 - 1.32858\,t$$

$$\phi R = 0.9 \times 9 \times 0.0008198 \times 413.793 = 2.74774\ M\ \ N\ (617.7k)$$

Setting ϕR equal to U and solving for t:

$$2.74774 = 4.15131 - 1.32858\ t$$

$$t = 1.0564 \text{ m } (3.465 \text{ ft}), \text{ Use } 1.067 \text{ m } (3.50 \text{ ft})$$

b. Thickness without anchors. From above

$$W_u = 2.5\,0\,4\,5\,6 + 0.82144\,t, \quad W_c = 1.97078\,t$$

From Chapter 3 for an *unusual* load condition, a *normal* structure, and *normal* site information the required factor of safety against flotation is FS = 1.20. Setting W_c equal to FS(W_u) and solving for t:

$$1.97078\,t = 1.20\,(2.50456 + 0.82144\,t)$$

$$0.98505\,t = 3.00547, \quad t = 3.051\,m\,(10.00\ ft)$$

c. Conclusion. This example illustrates the importance of untensioned structural anchors for slabs on grade subject to high uplift pressures. It is obvious from inspection that the anchored slab would be more economical, i.e., 1.067 m (3.5 ft) versus 3.051 m (10.0 ft) thick slab.

D-8. Example D8, Critical Slip Plane Angle (α) For An Earth Wedge With A Broken Top Surface

This driving-side wedge has a broken top surface, the water table lies within the wedge, and the soil possesses internal friction only, as shown in Figure D-18.

First, it is assumed that the top surface of the wedge is horizontal and lies along line ABC. Then the weight of the area BCD will be taken as an analogous negative strip surcharge (V). Where

$$V = -\frac{1}{2}(0.01886)(7.5)(3) = -0.212175\ M\ \ N\ /m\ \ [-14.53 \text{ k/ft}]$$

Since the water table lies within the wedge, the average effective unit weight of soil will be used in the calculations for the critical-slip plane angle.

$$\gamma = \gamma_{avg} = \gamma_m - \frac{(\gamma_m - \gamma_b)h_s^2}{h^2}$$

$$\gamma = 0.01886 - \frac{0.009\,0\,4\,(7)^2}{(18)^2} = 0.017493\ M\ \ N\ /\ m^3\ \ [0.11132 \text{ kcf}]$$

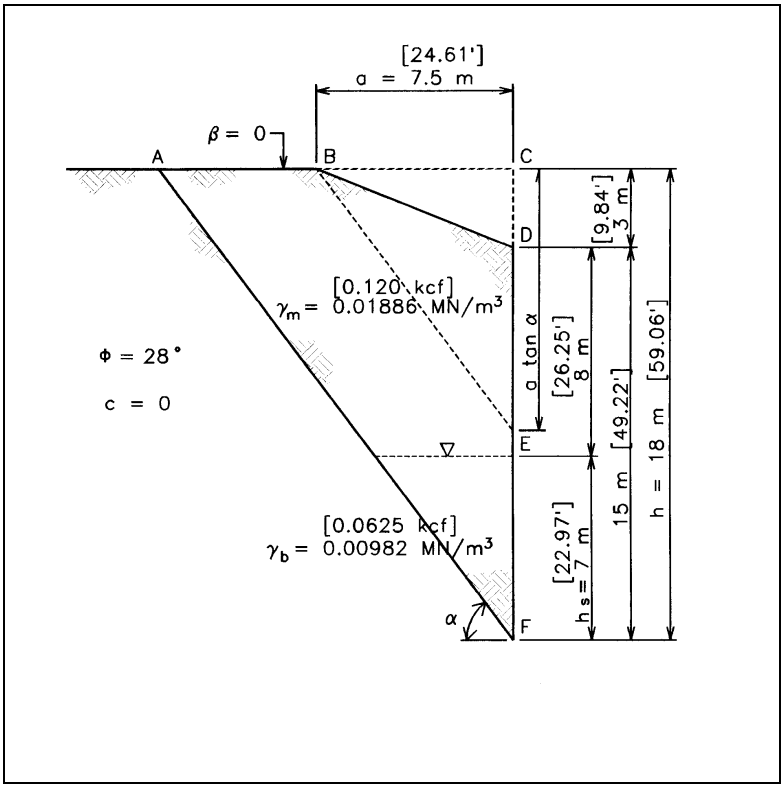

Figure D-18

Using the equations in Chapter 5, calculate the value of the critical-slip plane angle.

$$r = 1 - \tan\beta \tan\phi = 1 - 0 \times 0.531709 = 1.00$$

$$s = \tan\phi + \tan\beta = 0.531709 + 0 = 0.531709$$

$$t = \tan\phi - \tan\beta \tan^2\phi = 0.531709 - 0\,(0.531709)^2 = 0.531709$$

$$\alpha = \tan^{-1}\left(\frac{C_1 + \sqrt{C_1^2 + C_2^2}}{2}\right) = 55.8637^0$$

$$C_1 = \frac{2\,s \tan\phi}{A} = \frac{2 \times 0.531709 \times 0.531709}{0.627747} = 0.900727$$

$$C_2 = \frac{t}{A} = \frac{0.531709}{0.627747} = 0.847012$$

$$A = s - \left(\frac{2V}{\gamma h^2}\right)(1 - \tan^2\phi) = 0.531709 - \left(\frac{-2 \times 0.212175}{0.017493\,(18)^2}\right)(1.2182714) = 0.627747$$

D-9. Example D9, Critical Slip Plane Angle (α) with Cohesive Soil

The wedge in this example is the same as the wedge in Example D8, except that the soil possesses cohesive strength as well as internal friction, as shown in Figure D-19.

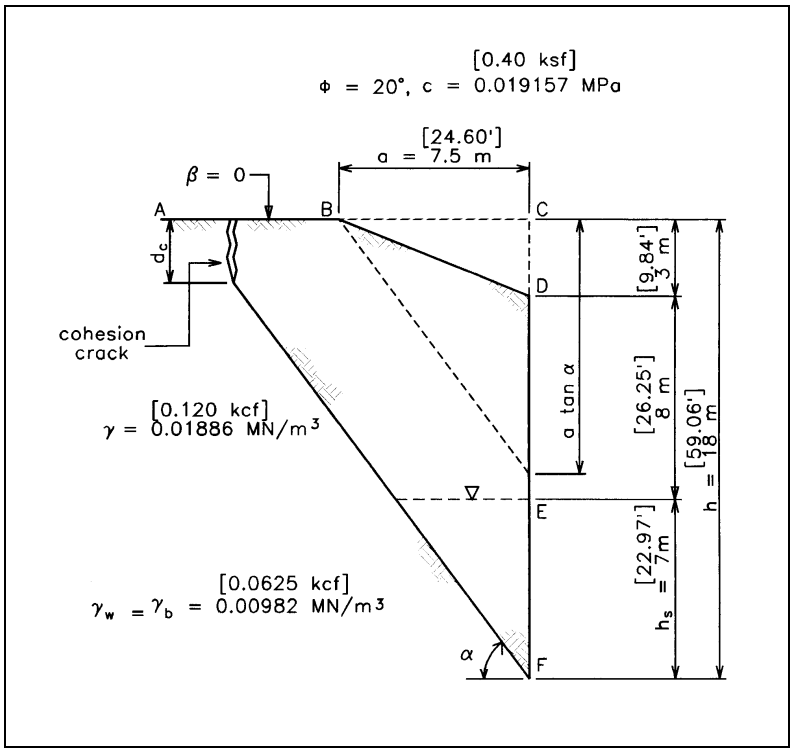

Figure D-19

Again, it is assumed that the top surface of the wedge is horizontal and lies along the line ABC. The weight of the area BCD will be taken as an analogous negative surcharge load (*V*).

Where

$$V = -\frac{1}{2}(0.01886)\ (7.5)\ (3) = -0.212175\ \ M\ \ N\ \ /m\ \ [\ 14.53\ \text{k/ft}\ ]$$

Since the water table lies within the wedge, the average effective unit weight of soil will be used in determining the critical slip plane angle for the wedge.

$$\gamma = \gamma_{avg} = \gamma_m - \frac{(\gamma_m - \gamma_b)\,h_s^2}{(h^2 - d_c^2)}$$

Since the depth of cohesive cracking (d_c) is not known initially, it must be estimated at the start and the equations in Chapter 5 used in an iterative fashion until the critical-slip plane angle (α) is found that produces a calculated value for crack depth that is equal to the estimated value.

$$r = 1 - \tan\phi \tan\beta = 1.00$$

$$s = \tan\phi + \tan\beta = 0.36397$$

$$t = \tan\phi - \tan\beta \tan^2\phi = 0.36397$$

1st Trial: estimate dc = 3 m

$$\gamma = \gamma_{avg} = 0.01886 - \frac{0.00904\ (7\ )^2}{(18\ )^2 - (3\ )^2} = 0.017454\ M\ \ N\ /\ m^3\ [0.11107\ \text{k/ ft}^3]$$

$$\gamma\ (h^2 - d_c^2)\ = 5.49801,\ \ \gamma\ (h + d_c) = 0.366534$$

$$A = s - \left(\frac{2V}{\gamma\ (h^2 - d_c^2)}\right)(1 + \tan^2\phi) + \left(\frac{2c}{\gamma\ (h + d_c)}\right) r$$

$$A = 0.36397 - \left[\frac{2\ (-0.212175\ )}{5.49801}\right](1.132474)\ + \left(\frac{2\ x\ 0.019157}{0.366534}\right)(1.00) = 0.555908$$

$$C_1 = \frac{2\ s \tan\phi + \left(\frac{4c}{\gamma\ (h + d_c)}\right) s}{A}$$

$$C_1 = \frac{2\ (0.36397)\ (0.36397)\ + \left(\frac{4\ x\ 0.019157}{0.366534}\right)(0.36397)}{0.555908} = 0.613483$$

$$C_2 = \frac{t + \left(\frac{2c}{\gamma\ (h + d_c)}\right) r}{A}$$

$$C_2 = \frac{0.36397\ + \left(\frac{2\ x\ 0.019157}{0.366534}\right)(1.00)}{0.555908} = 0.842766$$

$$\alpha = \tan^{-1}\left(\frac{C_1 + \sqrt{C_1^2 + 4\,C_2}}{2}\right) = 51.885°$$

Calculate d_c and compare to the initial estimated value.

$$d_c = \frac{2\,K_c\,c}{K\,\gamma_m},\ K = \frac{1 - \tan\phi \cot\alpha}{1 + (\tan\phi)\tan\alpha} = 0.488038$$

$$K_c = \frac{1}{2 \sin\alpha \cos\alpha\ [\ r + s \tan\alpha\ ]} = 0.703303, d_c = \frac{2\ x\ 0.703303\ x\ 0.019157}{0.488308\ x\ 0.01886} = 2.93\ m$$

This is so close to the estimated initial value that further iteration is not necessary, and $\alpha = 51.9^{o}$.